PERSPECTIVE

Misery Perfusion, Diffusive Oxygen Shunting and Interarterial Watershed Infarction Underlie Oxygenation-Based Hypoperfusion Maculopathy

DAVID MCLEOD

• PURPOSE: To describe and explain the entire range of acute ischemic macular damage that follows panretinal hypoperfusion from central retinal artery or vein occlusion.
• DESIGN: Perspective article.
• METHODS: To correlate the fundoscopic, fluorescein angiographic, oximetric, and optical coherence tomographic (OCT) features developing within the posterior inner retina following incremental reductions in arteriovenous perfusion pressure across the retinal circulation.
• RESULTS: The spectrum of acute oxygenation-based hypoperfusion maculopathy (OHM) is consistent with that predictable from a modified Krogh cylinder model of tissue oxygenation. Diffusive oxygen shunting plays a significant role in the "artery-dominated" generation of ischemic signs during misery perfusion. Three major grades of OHM severity can be discerned according to the predominant oxygenation status of ganglion cells within the superficial inner retina, whether this is normoxic (OHM1), hypoxic (OHM2), or anoxic (OHM3). Densely opaque axoplasmic sentinels are arranged along normoxic/hypoxic interfaces in OHM2. In OHM1 and OHM2, relative hypermetabolism and interarterial watershed infarction of fundal interneurons (WIFI) underpin subtle middle-retinal opacification with periarterial sparing. The fundal signs are optimally displayed en face using autofluorescence imaging whereas cross-sectional OCT reveals Paques' plaque formation.
• CONCLUSIONS: An exquisite and supremely accessible exhibition of classical oxygen physiopathology unfolds in eyes with panretinal hypoperfusion courtesy of the transparent ocular media and the pattern of macular neuroretinal opacification that evolves as upstream tissues extract oxygen to the detriment of tissues downstream. Recent attempts to overrule the simple conceptual framework embodied in WIFI have no plausible anatomical nor physiological basis. Overreliance on OCT can result in misdiagnosis. (Am J Ophthalmol 2019;205:153–164. © 2019 Elsevier Inc. All rights reserved.)

IN 1859, ALBRECHT VON GRAEFE DESCRIBED THE DIFFUSE inner retinal opacification and foveolar cherry-red spot formation that follows complete occlusion of the central retinal artery (CRA). It was not until 1978, however, that the heterogeneous fundal signs associated with a lesser degree of panretinal hypoperfusion were recognized, illustrated, and interpreted.

MODERATELY SEVERE HYPOPERFUSION MACULOPATHY

IN EYES WITH PARTIAL CRA OCCLUSION (CRAO), THE POSTERIOR retina exhibits subtle opacification (ostensibly signifying a reduced thickness of tissue infarction) accompanied by periarterial sparing.[1,2] Thus, tapering retinal transparency surrounds the macular arteries (n = 7–9) as they converge toward an ill-defined cherry-red spot. Alternatively termed the "arteriae afferentes of His" or "terminal" arteries, these second-order arteries alternate with the macular veins in a radiating pattern. As well as giving off several (first-order) precapillary arterioles as side branches, they often branch dichotomously having earlier arisen orthogonally from the main branchings of the CRA. The latter (third-order) retinal arteries otherwise branch dichotomously and have a

AJO.com Supplemental Material available at AJO.com.

Accepted for publication Mar 9, 2019.

From the Academic Department of Ophthalmology, Manchester Royal Eye Hospital, Manchester University National Health Service Foundation Trust, and Centre for Ophthalmology and Vision Research, Institute of Human Development, University of Manchester, Manchester, United Kingdom.

Inquiries to David McLeod, Academic Department of Ophthalmology, Manchester Royal Eye Hospital, Manchester University NHS Foundation Trust, Oxford Road, Manchester M13 9WL, United Kingdom; e-mail: david.mcleod@nhs.net

0002-9394/$36.00
https://doi.org/10.1016/j.ajo.2019.03.015

trajectory that mirrors that of axon bundles within the retinal nerve-fiber layer (NFL).[3,4] Of note, in this pragmatic ascending 3-step hierarchy that encompasses the entire intraocular CRA tree, those afferent vessels that can be resolved ophthalmoscopically are referred to here as "arteries" despite their small size and absent internal elastic lamina (as tradition holds).

Differentiation between translucent and transparent retina by standard ophthalmoscopy has always been challenging (Figure 1) but, in recent years, fundus autofluorescence (FAF) imaging has proved invaluable in precisely delineating the ischemic topography.[5] Useful semiquantitative data for the perfusion failure underlying this topography are furnished by fundus fluorescein angiography (FFA) through analysis of the delay in dye filling of the arteries and the very prolonged dye transit (Figure 1). However, many consider the utility of FFA in ischemia assessment to be limited by its inability to depth-resolve the retinal capillary network. By contrast, optical coherence tomography (OCT) angiography displays blood circulation within all 3 interconnecting microvascular strata in the macular region (ie, the deep capillary plexus [DCP] and intermediate plexus, now known collectively as the deep vascular complex [DVC], together with the superficial capillary plexus [SCP]).[6,7] As such, OCT angiography is said to offer distinct benefits over FFA in elucidating the physiopathology of retinal ischemia, but this view presupposes that the damage mechanisms hinge on the finer details of retinal microvascular anatomy (which is not necessarily the case).

Typically, macular retinal translucency with periarterial sparing in partial CRAO is accompanied by multiple cotton-wool spots (CWSs) in an annulate peripapillary distribution.[1,2] This may include small CWSs lying embedded within the hypoperfused macula in the fork of an arterial bifurcation or at other locations where the trajectories of arteries and axon bundles diverge (Figure 1). These densely opaque lesions reflect obstruction of the retrograde transportation of mitochondria within the axoplasm of unmyelinated retinal ganglion-cell (RGC) axons. This mechanism can be envisioned as a deferral into the retina of the retrograde transport block often seen at the edge of the optic disc after complete CRAO. There, the localized "peripapillary axoplasmic ring" delineates a normoxic/anoxic interface within the optic nerve-head, whereas the multiple CWSs (or "axoplasmic sentinels") that evolve after partial CRAO appear along normoxic/hypoxic interfaces within the NFL.[4]

Modest, incompletely reversible visual loss, a relative afferent pupillary defect (RAPD) and retinal venous hypoxemia complete a multifaceted acute presentation that is entirely attributable to a single vascular occlusive event (ie, partial CRAO).[1] However, the CWSs are widely misinterpreted as focal "NFL infarcts" resulting from incidental occlusion of small, superficial end-vessels (rather than axoplasmic sentinels),[8–10] while the constellation of fundal signs is incorrectly ascribed to "transient CRAO" in the Iowa CRAO classification.[8] A similar reduction in the arteriovenous (AV) perfusion pressure across the retinal circulation can follow severe acute central retinal vein occlusion (CRVO) and will prompt the same pathological response.[1,11] However, only the larger axoplasmic accumulations escape obscuration by retinal hemorrhage in such circumstances.

MISERY PERFUSION, THE KROGH CYLINDER, THE ISCHEMIC PENUMBRA, AND WATERSHED INFARCTION

THE PHYSIOPATHOLOGICAL PROCESS INITIALLY PROPOSED to explain the ischemic damage following partial CRAO was preferential proximal oxygen extraction from the residual trickle of blood flowing through the inner retina.[1] Happily, this mechanistic hypothesis has stood the test of time, and neurologists have given the epithet "misery perfusion" to similar ischemic episodes within the brain wherein, despite an overall reduction in oxygen delivery, oxidative metabolism continues unabated in those tissues that have priority access to the oxygen supply.[12] This "first-come, first-served" upstream provision proceeds regardless of the consequences for more distally located cells within the hypoperfused vascular territory. The oxygen extraction fraction increases from its usual value (35–45%) to 100% as blood reaching the downstream portion of the vascular pathway becomes entirely oxygen desaturated.[4,12,13] This supply deficit is demonstrated in the retina by the marked venous darkening.

In appropriate circumstances (such as those to be found within the posterior polar retina), the detailed ischemic geography associated with misery perfusion can be explained by the century-old "Krogh cylinder" model of tissue oxygenation.[4,14,15] This model consists of a regularly spaced 3-dimensional (3D) array of parallel capillaries that Krogh designed to simulate oxygen convection within skeletal muscle, with subsequent oxygen diffusion into the parenchyma.[14] Each capillary derives from division of the same precapillary arteriole and exclusively oxygenates a concentrically surrounding sleeve of cells with uniform mitochondrial density before reuniting with the other capillaries to form a postcapillary venule (Figure 2). Within each tissue cylinder, oxygen diffuses radially down a parabolic oxygen tension (pO_2) gradient between the "oxygen pressure head" (ie, the intravascular pO_2 maximum) within the axial capillary and the circumferential "oxygen watershed" (ie, the aligned tissue pO_2 minima) where neighboring cylinders abut one another. The linear reduction in oxyhemoglobin (HbO_2) saturation along the capillaries translates (through the local HbO_2 dissociation curve) into decreasing pO_2

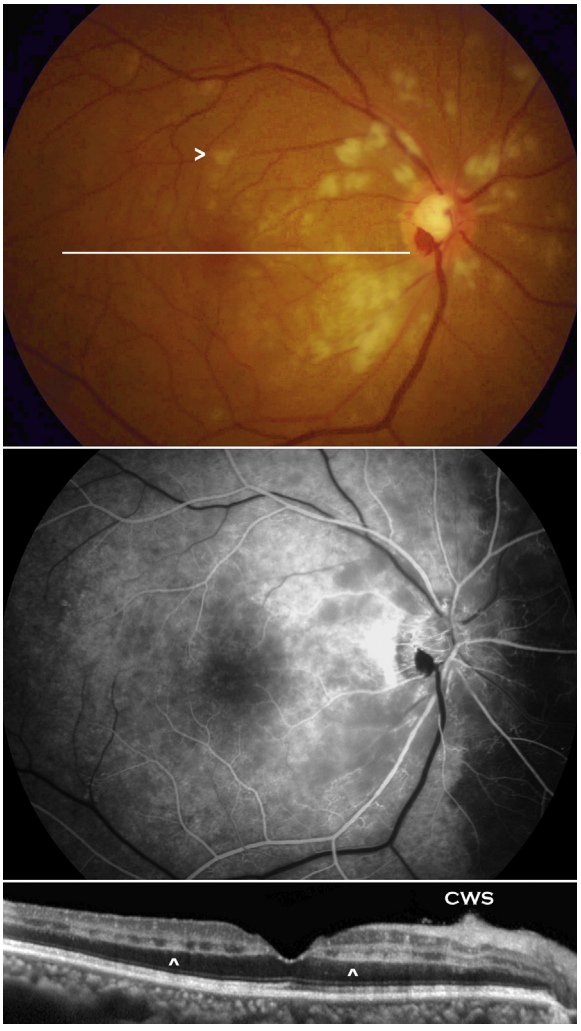

FIGURE 1. Photographic, fundus fluorescein angiographic (FFA), and optical coherence tomographic (OCT) studies from a 68-year-old patient presenting with partial central retinal artery occlusion or oxygenation-based hypoperfusion maculopathy grade 2 (courtesy of Prof. Se Joon Woo, Seoul, South Korea). (Top) Color photography shows heterogeneous fundal opacification including macular translucency with periarterial transparency and opaque cotton-wool spot (CWS) formation in an "annulate" distribution pattern around the optic disc. An embedded axoplasmic sentinel (>) is seen within the ischemic retina above the fovea (acuity = counting fingers). Retinal venous hypoxemia signifies misery perfusion. The white horizontal line indicates the location of the optical coherence tomography (OCT) B-scan section shown below. (Middle) The FFA view taken at 40 s from dye injection shows slow filling of the retinal arteries but no venous filling, even at this late stage. Delayed choroidal filling nasally suggests an associated medial posterior ciliary artery occlusion. Masking of the underlying choroidal fluorescence in precise relation to the axoplasmic sentinels is often misinterpreted as evidence of focal end-vessel occlusion. (Bottom) Horizontal OCT B-scan section in the plane of the fovea shows Paques' plaques (ie, placoid hyperreflectivity of the inner nuclear layer (^) with periarterial sparing, otherwise called interarterial watershed infarction of fundal interneurons). The normal, layered structure of the inner retina is preserved but a relatively small axoplasmic sentinel (CWS) expands the nerve-fiber layer into the vitreous and distorts the subjacent lamellae.

maxima driving the radial diffusion, with consequent lowering of tangential pO_2 profiles downstream (Figure 2).

With incremental perfusion failure, these tangential pO_2 profiles are further lowered pari passu, and the oxygen supply to cells is first exhausted (and tissue infarction commences) at the venous end of each capillary toward the cylinder circumference ie, in the so-called "anoxic corner" or "lethal corner" of the Krogh cylinder.[14,15] Adjacent anoxic corners from neighboring tissue cylinders then progressively and symmetrically span the oxygen watersheds, the intercapillary "interterritorial" or "watershed" infarction reflecting collective diminution of blood flow through vessels that share a common parent source located some distance proximally (Figure 2). This mechanism contrasts with the focal (or "pan-territorial") infarction that follows total occlusion of a local end-vessel; however, watershed infarction also progresses to confluent necrosis as surviving pericapillary cells taper to nothing. Of note, in neither case does the venous topology influence the infarct topography.

The original Krogh cylinder model implicated only 2 tissue oxygenation states (ie, normoxia and anoxia) above and below a single critical tissue pO_2 threshold. Within neural tissue, however, Symon's dual threshold paradigm dictates that an intermediate oxygenation state called the "ischemic penumbra" will arise as parenchymal perfusion diminishes.[4,16,17] This hypoxic tissue compartment is bounded by critical pO_2 isobars for hypoxia (probably at $\approx$10 torr) and anoxia (at 1–2 torr). In the Krogh model, therefore, a "hypoxic funnel" of neurons must be intercalated between the tapering pericapillary sleeve of normoxic cells and the cylinder's anoxic corner (Figure 2).[4,15]

Hypoxic neurons are functionally impaired or electrically silent (ie, synaptic and axonal conduction is suspended), but the cells' resting membrane potential is nevertheless maintained (so-called ionic homeostasis). This suppression of metabolic demand from ion pumping serves to protect the cells' integrity (ie, the neurons remain structurally intact).[17] Within the retina, for example, optical transparency and OCT reflectivity are apparently unaffected by hypoxia as thus defined, and visual function can improve within minutes of reperfusion and tissue reoxygenation (eg, after CRA recanalization by local intra-arterial fibrinolysis).[4] The generation of ATP is also much reduced within these hypo-oxygenated cells, but this limited production is in balance with ATP utilization (so-called energy homeostasis). Protein synthesis diminishes as part of this adaptive mechanism, but essential vegetative processes continue, including exaggerated expression

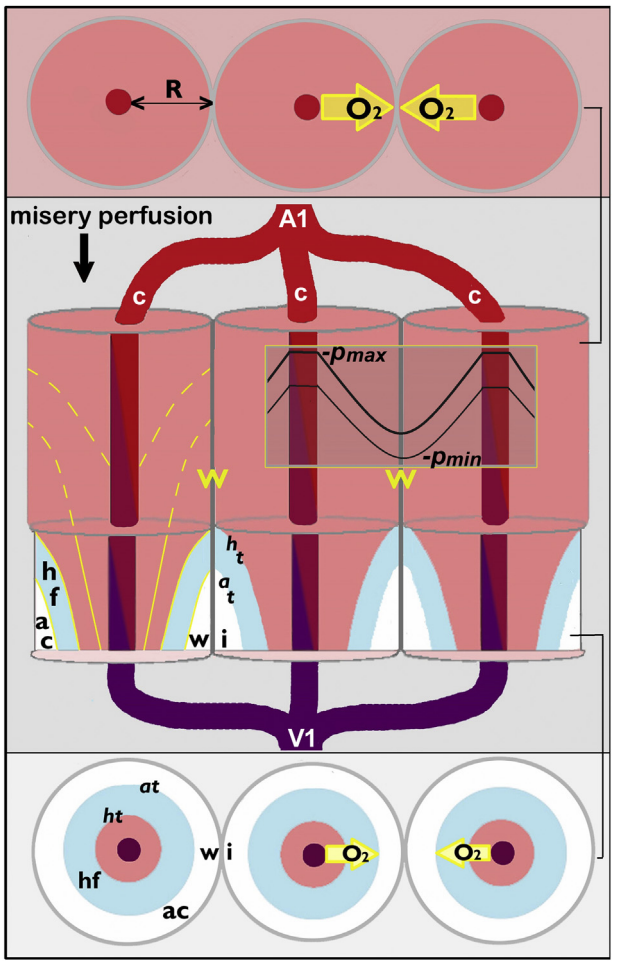

FIGURE 2. Color-coded Krogh cylinder model demonstrating the mechanism of intercapillary watershed infarction. Three adjacent tissue cylinders from a larger volume of hypoperfused neural parenchyma are shown, together with cross-sections through their proximal (above) and distal (below) ends. The tissue cylinders are concentric to parallel capillaries (c) organized in a regular array. The capillaries branch from the same (first-order) precapillary arteriole (A1) and then reunite to form a postcapillary venule (V1). Blood flow is thus concurrent. In reality the length of the tissue cylinder relative to its radius is 10 to 20 times that shown. The sleeves of parenchyma have a uniform mitochondrial density and comprise normoxic (pink shading), hypoxic (pale blue shading), or anoxic (unshaded) cells. In the proximal section, oxygen is shown diffusing radially (yellow arrows) from the capillaries toward the cylinder circumference. "R" denotes the cylinder radius. Oxygen flux becomes zero at the midway point between neighboring capillaries. Oxygen saturation within the axial blood columns decreases linearly, as indicated by the color change from red to purple (ie, "misery perfusion"). Representative oxygen tension (pO_2) isobars within the cylinder on the left are shown as continuous or dashed yellow contour lines. Serial pO_2 profiles in the gray box overlying the 2 cylinders on the right are not on the same y-axis or scale as these isobars. p_{max} is the intracapillary pO_2 maximum on the upper profile, and p_{min} is the tissue pO_2 minimum on the lower profile. The location of the intercapillary "oxygen watershed" (ie, the aligned pO_2 minima) along the interface between adjacent tissue cylinders is marked by a yellow W. The cutaway vertical section and the horizontal section through the distal part of each cylinder (below) show tapering normoxic pericapillary tissue giving way to a concentric funnel of hypoxic parenchyma. This "hypoxic funnel" (hf) is delineated by pO_2 isobars representing Symon's hypoxia threshold (*ht*) and anoxia threshold (*at*). Anoxic tissue bordering the circumference and base of each cylinder forms an "anoxic corner" (ac) consisting of neurons that are most vulnerable to ischemia by virtue of their distal location. Where tissue cylinders and their anoxic corners are in apposition, the combined anoxic zone spanning the oxygen watershed represents intercapillary watershed infarction (wi) with pericapillary sparing.

of neuroprotective and angiogenic proteins such as vascular endothelial growth factor. Of note, such penumbral "hypometabolism" lessens the slope of pO_2 gradients generated within the hypoxic tissue, so the diffusion distance for oxygen is extended and the volume of infarction is reduced.[15]

MACULAR NEUROVASCULAR PHYSIOPATHOLOGY IN THE PLANE OF THE RETINA

THE KROGH CYLINDER MODEL RELATES PERFECTLY (OR almost perfectly) to in vivo macular retinal oxygenation as follows.[4,15] First, the macular arteries can replace the model's axial capillaries, given their free oxygen-permeability (witness the periarterial capillary-free zone of His) and their appropriate (ie, parallel or converging) 2D geometry. Radial oxygen movement between the axial arteries and interarterial oxygen watersheds then takes place by "diffusive oxygen shunting", oxygen molecules following the pO_2 gradients generated by mitochondrial metabolism instead of faithfully tracking the flow of erythrocytes along a sequence of microvessels (Figure 3).[4,18] Capillary distribution and orientation have only limited influence over parenchymal oxygenation, therefore.

Second, as the Krogh model requires, the inner retinal lamellae each have a uniform mitochondrial density in the horizontal plane, at least for the 100 to 200 μm distances relevant to this tissue geometry. This is demonstrable by mitochondrial enzyme histochemistry and also by the even lamellar reflectivity normally observed on cross-sectional OCT (as with the photoreceptor ellipsoid band in the outer retina).[4,19,20] Thus, mitochondria have the appropriate size, shape, and refractive index (ie, 1.4) to dominate determination of lamellar OCT reflectivity. The greatest mitochondrial densities in the inner retina are evident within the plexiform layers and NFL (albeit not so dense as within the ellipsoid layer). The lowest density is to be found within the inner nuclear layer

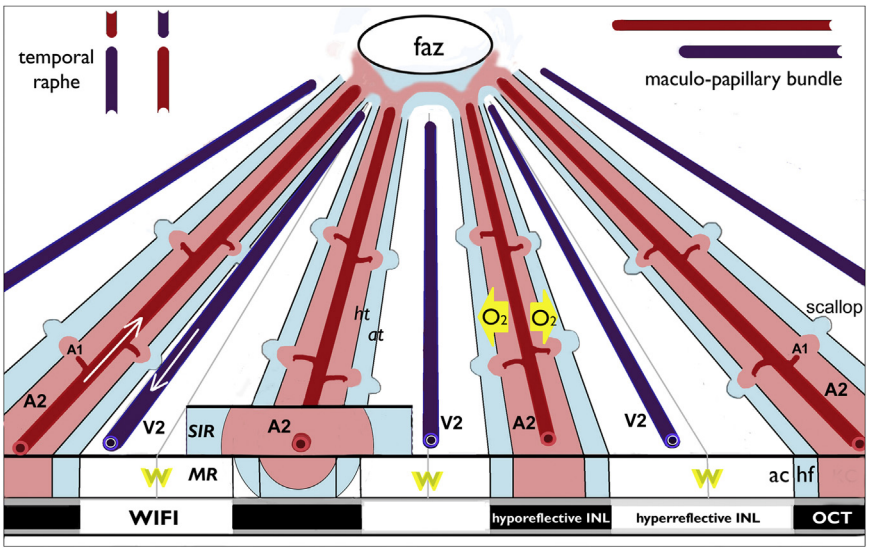

FIGURE 3. Schematic color-coded depiction of middle retinal (MR) oxygenation in the inferior macula during panretinal hypoperfusion of moderate severity. The corresponding optical coherence tomographic (OCT) B-scan features are shown beneath in black and white. Radiating around the foveal avascular zone (faz) are second-order arteries (A2) that course within the superficial inner retina (SIR), as shown in the small inset. The A2 arteries alternate with macular veins (V2) that contain oxygen-desaturated blood. White arrows indicate countercurrent blood flow. The A2 arteries give off (first-order) precapillary arterioles (A1) orthogonally. This A1 branching is staggered and, for the sake of clarity, only 4 arterioles per artery are shown (instead of 8 or more). No A2 bifurcations are shown and neither is the capillary network. Surviving MR tissue, consisting of normoxic (pink shading) and hypoxic (pale blue shading) interneurons, shows "reflectional" or "axial" geometric symmetry with respect to the overlying A2 arteries and tapers toward the faz. Yellow arrows indicate the predominant (radial) direction of diffusive oxygen shunting. Anoxic interneurons (unshaded) have no specific spatial relation to the V2 veins except where a vein's course happens to coincide with an oxygen watershed (yellow W on a thin gray line), as shown in the central portion of the diagram. Infarction spanning the oxygen watersheds comprises the combined anoxic corners (ac) of adjacent Krogh cylinders based on the A2 arteries. The margins of the hypoxic funnel (hf) correspond to pO_2 isobars representing Symon's hypoxia threshold (*ht*) and anoxia threshold (*at*). The infarct margins are scalloped in relation to the A1 branchings as they dive into the middle retina. On cross-sectional OCT (below), the inner nuclear layer (INL) remains hyporeflective in normoxic and hypoxic environments, whereas anoxic INL becomes hyperreflective (Paques' plaque formation) and represents interarterial watershed infarction of fundal interneurons (WIFI).

(INL), whereas an intermediate level is apparent within the RGC layer.

Given this vertical inhomogeneity in lamellar mitochondrial density, the steepness of pO_2 gradients generated by neuronal metabolism will vary with retinal depth (see discussion below). However, in the horizontal plane, the interarterial location of the oxygen watershed is the same across the entire thickness of the inner retina because metabolic demand within each individual lamella is homogeneous. The watershed sits precisely midway between neighboring macular arteries that arise by truly dichotomous division (mirroring the Krogh model) or approximately midway otherwise (Figure 3). After upscaling from the capillary to the arterial level, therefore, the effective radius of tissue cylinders in the horizontal plane is one-half (or roughly one-half) the interarterial distance.

Misery perfusion of the inner retina, reflecting residual flow following either CRVO or CRAO, will then result in anoxic corner formation and *interarterial* watershed infarction with periarterial sparing. The severity of ischemia determines the relative proportions of normoxic, hypoxic, and anoxic tissue volumes that arise, the pattern of second-order arterial branching providing the template for these oxygenation-based tissue compartments (as documented diagrammatically in Figure 3). The symmetrical tapering of transparent (ie, normoxic and hypoxic) parenchyma implicates an artery-dominated physiopathology, the macular veins merely occupying the same interarterial space as the opacified and hyperreflective anoxic tissue unless the course of a vein coincidentally coincides with the alignment of tissue pO_2 minima (see discussion below).[4] Occasionally, infarction localizes to the temporal horizontal raphe, and here it represents watershed infarction between third-order vessels (ie, between the major branches of the CRA tree).[15,21,22] A similar influence underlies the predilection of infarction for the temporal half of the macula (Figure 4).

MILD HYPOPERFUSION MACULOPATHY

TWO FURTHER DISCOVERIES WERE TO HELP CEMENT A comprehensive conceptual framework for the ischemic maculopathy that follows panretinal hypoperfusion. First, a forme fruste of the partial CRAO picture was reported in 2002-2003 in eyes with moderately severe CRVO and significant retardation of the dye transit on FFA. The undramatic fundal signs comprise retinal translucency with periarterial sparing (as in partial CRAO) but with no annulate or artery-related CWSs and no detectable RAPD (Figure 4).[21,22] The absence of ischemic damage within the superficial inner retina (SIR) implies a lesser severity of misery perfusion with a legacy of paracentral scotomata but with no optic atrophy or NFL grooves (unlike after partial CRAO). Although accelerated HbO_2 desaturation was properly proposed as the ischemic mechanism in these CRVO eyes; however, the lowest tissue pO_2 values were presumed to be located close to the macular veins.[21,22] Thus, the infarction was portrayed as "perivenular" (a topographic expression of convenience) instead of interarterial and interterritorial. The anoxic damage was also described as "fern-like" (ie, axially symmetrical about the veins). On the contrary, the geometric symmetry is explicitly about the arteries.

Second, using high-resolution OCT, Michel Paques from Paris, France was the first to confirm the depth localization of infarction to the middle-retinal (MR) lamellae in such CRVO cases. The most obvious manifestation is the conversion from normal INL hyporeflectivity to anoxic hyperreflectivity, changes in the already hyperreflective plexiform tissues being less readily characterized (Figure 4). Best seen in OCT sections that cut across the macular vessels, periarterial sparing subdivides the interneuron infarction into "skip lesions" or "Paques' plaques". Within a few weeks from ischemia onset, however, neuroretinal transparency is restored, but OCT signs of INL atrophy become evident, the persistence of the ganglion-cell complex (GCC) and photoreceptor cells confirming that the interneurons had indeed borne the brunt of the acute ischemia. Publication of a series of these cases foundered in 2008, so dissemination of Paques' findings was delayed.[23]

The interarterial infarction resulting from moderate panretinal hypoperfusion, and exclusively involving the MR, has now been given the mechanistically-appropriate title of "watershed infarction of fundal interneurons" (WIFI). Because different subregions of individual retinal neurons (and not least the bipolar interneurons) may have differential access to oxygen resources, intracellular energy transfer (through the phosphocreatine shuttle, for example) probably determines the survival or otherwise of progressively hypo-oxygenated cells.[24] This likely accounts for the clear delineation of tissue infarction usually apparent on FAF and OCT imaging of WIFI.

MACULAR NEUROVASCULAR PHYSIOPATHOLOGY IN THE TRANSRETINAL PLANE

DURING PANRETINAL HYPOPERFUSION, THE RETINAL CAPILlary bed can be anticipated to become maximally and uniformly dilated as part of the vascular autoregulatory response. When considering the physiopathology of WIFI, therefore, there is no a priori reason to suppose that a significant difference in perfusion capacity exists between the SCP within the SIR and the DVC within the MR. This is not withstanding the varying metabolic environments extant within the various inner retinal tissue compartments. However, the simple (anatomical) fact remains that the second-order macular arteries and veins occupy the SIR to the exclusion of the MR.

Michaelson[3] regarded the deeper vascular strata as subsidiary to the superficial microcirculation by virtue of the developmental origins of the DVC from the SCP and the extended capillary pathway arising thereby. However, diffusive oxygen shunting dictates that oxygen movement down pO_2 gradients is largely independent of the minutiae of retinal microvascular anatomy, so "subsidiarity" of the MR microcirculation can be legitimately reinterpreted as a somewhat longer diffusion distance for oxygen between the macular arteries and the parenchymal mitochondria of the MR (compared with the SIR mitochondria). In support, Linsenmeier has observed that the transretinal (or retinochoroidal) pO_2 profile typically shows 2 inner retinal pO_2 peaks, of which the peak related to the DCP is slightly lower (ie, by $\approx$7 torr) than that related to the SCP.[25] Thus, courtesy of subsidiarity, the effective pO_2 maxima will be $\approx$ 7 torr lower within the MR than within the SIR (Figure 5).

In addition to MR/DVC subsidiarity, interneuron hypermetabolism (relative to GCC metabolism) appears to account for the exaggerated susceptibility of the MR to infarction. The high plexiform lamellar concentration of mitochondrial cytochrome oxidase (including enzyme located within the photoreceptor terminals) indicates increased metabolic demand from within the MR (relative to the SIR). Accordingly, pO_2 gradients will be steeper (as well as lower) within the MR, so Symon's thresholds for ischemic hypoxia and anoxia will be breached earlier, and interarterial watershed infarction will first and foremost involve the interneurons, as inner retinal perfusion progressively diminishes (Figure 5).

The oxygen watershed in question is an entirely separate entity from the pO_2 minimum on the transretinal pO_2 profile that some investigators regard as an

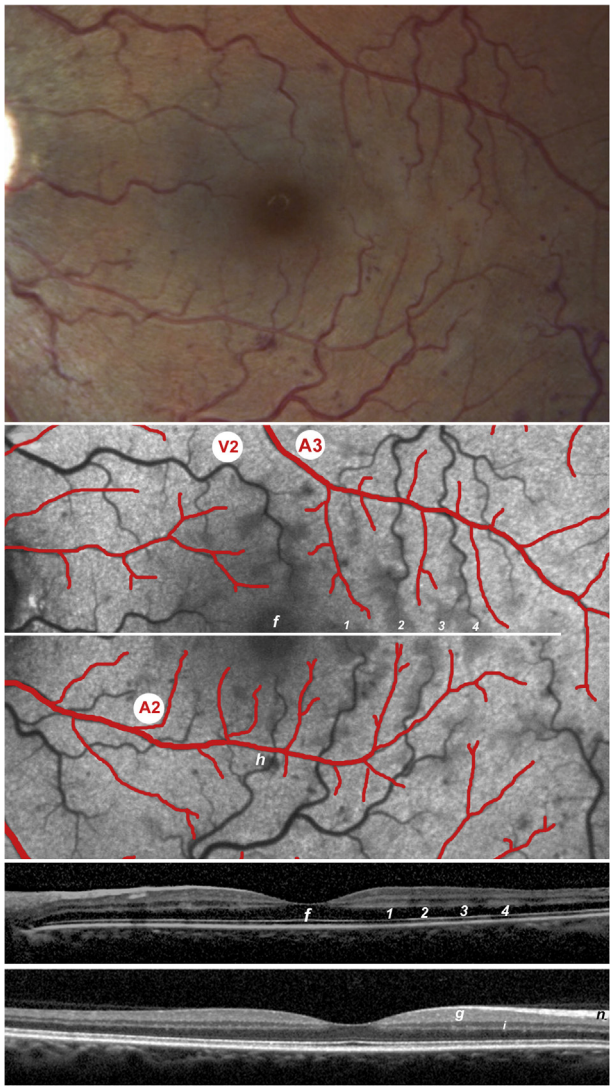

FIGURE 4. Photographic and optical coherence tomographic (OCT) studies of the left fundus of a 51-year-old patient presenting with central retinal vein occlusion at the tipping point between macular oligemia and ischemia (courtesy of Dr. Eduardo Cunha Souza, São Paulo, Brazil). (Top) Color picture of the central macular region undertaken 2 days after symptom onset shows venous tortuosity, a few blot and dot hemorrhages, and indiscrete patches of subtle retinal opacification (acuity = 20/80). (Middle) The fundus autofluorescence (FAF) image of the same field has been overlaid by a drawing of the arterial tree in red. Relatively straight second-order arteries (A2) arise more or less orthogonally from third-order branch arteries (A3) and alternate with tortuous second-order veins (V2) that appear black. Irregular dark gray lesions in the general vicinity of the veins represent masking of the normal silver-gray retinal pigment epithelial autofluorescence by intraretinal hemorrhages (h) or by interneuron infarcts such as those marked 1, 2, 3, and 4. There is temporal > nasal macular preponderance of infarction. Transparent retina spared from infarction lies symmetrically around the A2 arteries and tapers toward the foveola (f) or the temporal horizontal raphe. The dark gray lesions are narrower where the A2 arteries course close to one another and vice versa, and there is scalloping of infarct margins. Thus, the distribution of infarction respects the course of the arteries, not the veins (ie, the infarcts are interarterial, not perivenular). The white horizontal line indicates the plane of the corresponding OCT B-scan section below. (Bottom) OCT B-scans, the lower one taken from the normal fellow eye in which g = ganglion-cell layer, i = inner nuclear layer, and n = nerve-fiber layer. The upper scan from the affected eye demonstrates placoid hyperreflectivity of the inner nuclear layer (ie, Paques' plaques numbered as in the FAF study above) together with mild shadowing. The plaques represent interarterial watershed infarction of fundal interneurons.

important factor in the development of WIFI, otherwise known as "perivenular paracentral acute middle maculopathy" (pvPAMM).[10,26–30] The transretinal watershed is located in the region of the external limiting membrane and is primarily relevant to concomitant retinal and choroidal ischemia (eg, from carotid or ophthalmic artery stenosis) and not to isolated retinal hypoperfusion.[25] Conceivably, however, increased nocturnal oxygen demand by the photoreceptor ellipsoid will exacerbate an existential threat to the interneurons from MR hypo-oxygenation centered on the interarterial inner-retinal watershed.

OXYGENATION-BASED HYPOPERFUSION MACULOPATHY

A CONTINUOUS CLINICAL SPECTRUM OF OXYGENATION-based hypoperfusion maculopathy (OHM) is suggested by i) the depth localization of infarction to the MR in most CRVO cases, ii) the added involvement of the SIR in cases of partial CRAO (witness the CWSs and RAPD), and iii) the combined MR and SIR infarction arising after complete CRAO. Thus, although retinal blood volume flow rates can be difficult to quantify angiographically, the parenchymal consequences of panretinal hypoperfusion for the macular inner retina conveniently stratify the extent of perfusion failure courtesy of Symon's ischemia thresholds (ie, those determining the separation of normoxic from hypoxic and hypoxic from anoxic tissue compartments).[4,15,16]

The OHM spectrum primarily reflects the extent of perfusion failure and not the specific vessel implicated, whether the CRA or the central retinal vein. Nevertheless, by virtue of the multiple potential pathways for venous drainage even prior to occlusion, eyes with CRVO (which presents more frequently than CRAO) veer toward the mild end of the OHM spectrum.[5,21,22] By contrast, although examples of "occult CRAO" have been described,[10,28] eyes with CRAO are generally found toward the severe end owing to the limited potential for collateral flow circumventing complete CRAO or to

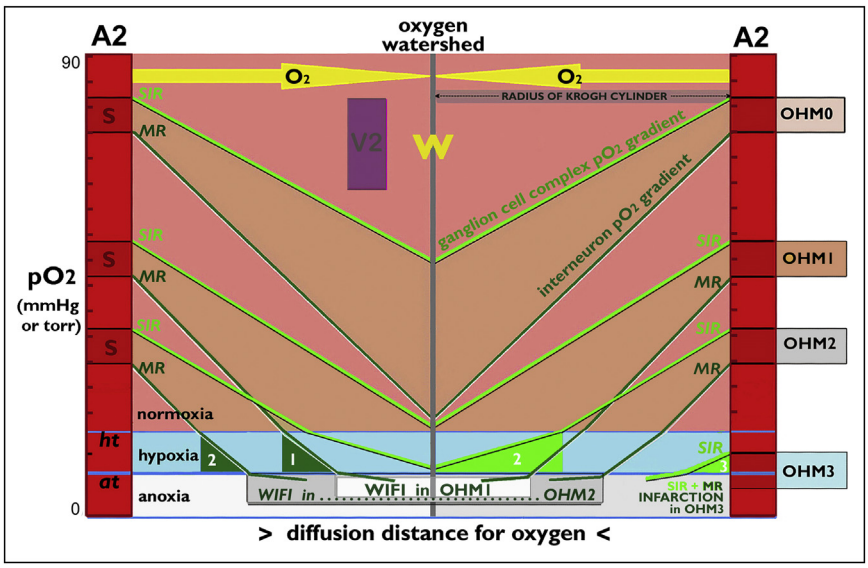

FIGURE 5. Diagram of the oxygen tension (pO_2) field between 2 second-order macular arteries (A2) arising dichotomously from a parent A2 artery (not shown) and illustrating 4 pairs of pO_2 profiles representing oxygenation-based hypoperfusion maculopathy (OHM) grades 1, 2, and 3, as well as the normal state (ie, OHM0). In OHM0, OHM1 and OHM2, the paired pO_2 profiles are each linked by a slight variation in pink shading. Each A2 artery is portrayed as a graduated "pO_2 burette" that dispenses oxygen into the superficial inner retina (SIR), consisting of the retinal ganglion-cell complex, and into the middle retina (MR), consisting of photoreceptor terminals and various types of interneuron. Because they are largely irrelevant to the model, other elements of the vascular compartment (such as capillary plexuses) are not shown apart from a second-order vein (V2) without graduation and in an arbitrary location. For the sake of clarity, pO_2 profiles emanating from the pO_2 maxima within the A2 arteries are shown as linear (rather than parabolic curves). The MR pO_2 gradients (dark green) are lower and steeper than the SIR gradients (bright green) by virtue of subsidiarity (S), as shown within the left A2 artery, and relative tissue hypermetabolism. The lowest pO_2 values (or tissue pO_2 minima) are to be found along the oxygen watershed located precisely midway between the arteries (gray line with yellow W). The aligned pO_2 minima also mark the point of apposition between the circumferences of Krogh tissue cylinders that, courtesy of diffusive oxygen shunting (yellow arrows), surround the A2 arteries. The location of the oxygen watershed bears no relation to the course of the V2 vein. The pO_2 field is partitioned horizontally into 3 color-coded oxygenation-based tissue compartments (ie, pink shading for normoxia, pale blue shading for hypoxia, and unshaded for anoxia) by means of pO_2 isobars representing Symon's hypoxia threshold (*ht*) and anoxia threshold (*at*). The lowest increment on the pO_2 scale may be logarithmic. All the tissue pO_2 gradients are parallel for the SIR and likewise for the MR. However, where a pO_2 profile crosses below *ht*, the slope becomes shallower (because hypoxic neurons are hypometabolic), and if *at* is crossed the gradient is shallower still. In OHM0, neither of the pO_2 profiles crosses *ht* nor *at*. In OHM1, only the interneuron profile crosses *ht* and *at*, and the resulting watershed infarction of fundal interneurons (WIFI) is displayed in a white box (marked "WIFI in OHM1") with an adjoining hypoxic compartment (dark green with a number 1 for OHM1) in the left half of the diagram. In OHM2, the pO_2 profile for the ganglion-cell complexes crosses *ht*, and the width of WIFI increases (pale gray box marked "*WIFI… in OHM2*"). The hypoxic SIR compartment spans the oxygen watershed (bright green with a number 2 for OHM2 in the right half of the diagram). In the left half, a hypoxic MR compartment adjoins WIFI (ie, dark green with a white 2). In OHM3, the pO_2 profiles for both the MR and SIR fall below *at*, thus indicating extensive infarction (white box across the entire interarterial width) apart from a tiny periarterial hypoxic SIR compartment (bright green with a number 3 for OHM3) reflecting a modicum of residual flow and shown solely on the right side of the diagram.

limited residual flow following incomplete luminal obstruction.

Grading of OHM severity is best achieved with reference to the oxygenation status of the SIR (Figures 5 and 6).[4,15] The designation OHM1 refers to normoxic SIR that occurs most frequently in association with moderately severe CRVO wherein ischemic change (hypoxic as well as anoxic) is restricted to the MR. However, eyes at this end of the OHM spectrum are particularly notable for offering crucial clinical evidence in support of the "misery perfusion" and "Krogh tissue cylinder" hypothesis. This is especially the case when noninvasive, artifact-free FAF imaging is used for ischemia assessment. Masking of retinal pigment epithelial autofluorescence by anoxic neuroretinal opacification provides an accurate and readily accessible display of the infarct topography.[5]

Thus, in eyes at the "tipping point" between macular oligemia (ie, OHM0) and mild macular ischemia (ie, OHM1), the tapering periarterial sparing, manifesting as MR transparency bordered by opacification (or by hypoautofluorescence), can be seen to be perfectly axially symmetrical (Figure 4). A minor exception to the 2D reflective

symmetry arises, however, where (first-order) precapillary arterioles branch orthogonally in the horizontal SIR plane from their parent (second-order) arteries before crossing the periarterial capillary-free zone and dividing into feeders for the SCP and DVC (the latter division "diving" into the MR).[3,7] This staggered precapillary arteriolar branching appears to be responsible for "scalloping" of infarct margins in an irregular arrangement (Figures 3 and 4).[5]

By contrast, the limited MR infarction arising at the tipping point has no consistent geometric relationship to the macular veins; it is as though the veins were not there (Figure 4). As noted earlier, the only circumstance in which the infarction is perivenular in strict geometric terms is when the vein's course happens to follow the interarterial watershed (Figure 3). Of course, this independence of the ischemic topography from the venous topology is less clearly apparent in eyes with more severe WIFI as the infarction comes to occupy more and more of the interarterial space, necessarily including the location of the alternating vein (Figure 6).

In OHM2, a predominantly hypoxic SIR is evidenced by the annulate distribution of axoplasmic sentinels ranging along normoxic/hypoxic interfaces, as seen most frequently in eyes with partial CRAO (Figure 1) but also, occasionally, after severe CRVO.[1,11] The associated RAPD reflects an expanded "polar penumbra" (ie, periarterial MR hypoxia with added SIR hypoxia in the posterior pole) that coalesces with an annular mid-peripheral hypoxic zone (the "penumbra obscura"), wherein nonperfused inner retina receives marginal oxygenation from the choroid sufficient to maintain tissue viability but insufficient to support pupillomotor activity.[4] The hypoxic SIR damage is potentially reversible, but it usually leaves a legacy of incomplete optic atrophy and/or CWS-based grooves in the NFL that appear to result from neurotrophic deprivation and intraretinal "compartment syndrome".[1,4,11]

Although OHM1 and OHM2 reflect differing degrees of perfusion failure (with a more prolonged and less pervasive dye transit on FFA in OHM2), the 2 OHM grades nevertheless exhibit similar OCT features (ie, Paques' plaque formation within the MR and normal SIR reflectivity except at the location of CWSs in OHM2 eyes). In failing to differentiate hypoxic from normoxic tissue, therefore, OCT only provides a limited characterization of ischemia severity and topography. It could also be that, for a given reduction in AV perfusion pressure, CRVO is more damaging to tissues than CRAO. This difference may relate to the myogenic component of the vascular autoregulatory response to venous occlusion (ie, the Bayliss effect).[31] Increased intramural oxygen consumption by hypertonic arteries after CRVO could lead to reduced radial oxygen diffusion and earlier evolution of anoxic corners.

In OHM3, which usually follows complete CRAO, both the MR and SIR are anoxic, opaque, and diffusely hyperreflective. However, in eyes with significant residual flow, symmetric RGC sparing may be found around the second- and third-order retinal arteries (Figures 5 and 6). Such periarterial SIR sparing is thought to account for the characteristic temporal peripheral visual field sparing that can accompany diffuse inner retinal infarction in the posterior pole despite its enveloping the optic disc.[4] A slightly greater extent of residual flow may permit periarterial sparing of full-thickness

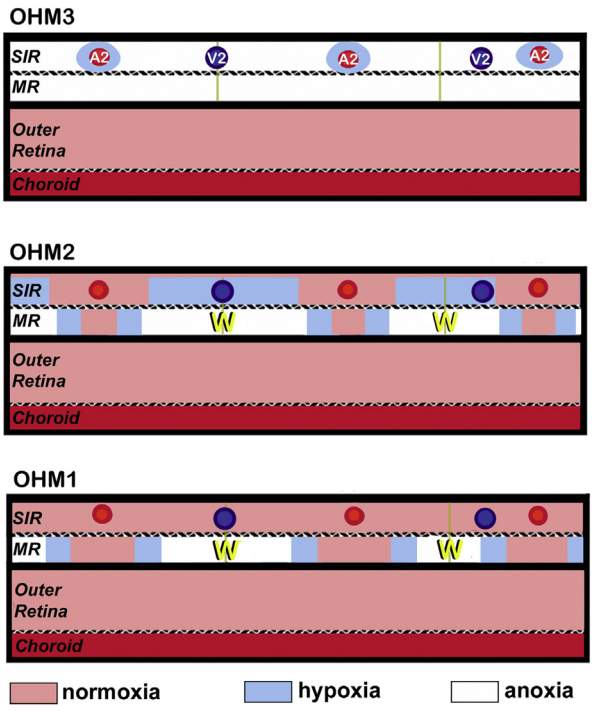

FIGURE 6. Schematic color-coded retinal sections cutting across 3 second-order macular arteries (A2) and 2 veins (V2). These sections portray the 3 grades of oxygenation-based hypoperfusion maculopathy (OHM) and the mechanism of watershed infarction of fundal interneurons. The OHM grade reflects the predominant oxygenation status of the superficial inner retina (SIR), whether normoxic (OHM1), hypoxic (OHM2), or anoxic (OHM3). The interarterial inner retinal oxygen watershed is shown as a vertical line with a yellow W. In OHM1 and OHM2, this watershed is straddled by anoxic infarction of the middle retina (MR). Each placoid MR infarct (or Paques' plaque) represents the conjunction of the anoxic corners of neighboring Krogh tissue cylinders. Interneuron infarction only respects veins with a course that coincidentally corresponds to the interarterial watershed (see left side of the diagram). Independence of MR infarction from the venous topology (right side of diagram) is more obvious in OHM1 than in OHM2. The width of MR infarction depends on the spacing between the arteries (compare left and right arterial pairings), as well as the OHM grade. Periarterial MR sparing is axially symmetrical and consists of both normoxic and hypoxic interneurons. In OHM3, the entire inner retina (ie, SIR + MR) undergoes anoxic infarction except where residual circulation permits periarterial SIR sparing.

FIGURE 7. Photographic and optical coherence tomographic (OCT) studies of the right fundus of a 54-year-old patient with central retinal artery occlusion and hand motion vision (courtesy of Prof. Se Joon Woo, Seoul, South Korea). (Top) Color photography undertaken 3 weeks after symptom onset shows extensive posterior polar opacification with a cherry-red spot and a tapering pattern of periarterial sparing of the superficial inner retina. The infarction has no specific spatial relationship to the second-order veins. Gross retinal vascular attenuation and retinal venous hypoxemia indicate residual misery perfusion. The white horizontal line indicates the location of the OCT section below. (Bottom) OCT B-scanning shows extensive inner retinal damage and progression to atrophy. There is confluent interneuron infarction and placoid ganglion-cell complex infarction ($_v$) with shadowing and periarterial sparing.

SIR throughout the macula on a background of confluent MR infarction (Figure 7). This ischemic topography reflects the same process and pattern of interarterial watershed infarction as that involving the interneurons in WIFI (Figure 5). However, although the GCC equivalent of Paques' plaques will be evident on cross-sectional OCT, there seems little likelihood that the geometrically inappropriate term "perivenular" will be attached to the SIR infarction.

PERIVENULAR PARACENTRAL ACUTE MIDDLE MACULOPATHY

IN 2014, PAQUES' PLAQUES WERE REDISCOVERED IN EYES with CRVO, and emphasis was placed on this OCT feature to the virtual exclusion of other indices such as oximetry and pupillary responses.[26] The isolated MR hyperreflectivity was given the descriptive but mechanistically-agnostic title of pvPAMM. Nevertheless, multifocal infarction from selective "ischemia of the DVC" (as distinct from ischemia of the SCP) was proffered as the cause,[10,26–30] apparently for want of a better explanation.[6] The implication, as expressed in the introduction to several reports, is that eyes with pvPAMM might showcase OCT angiography. On the contrary, it is here contended that the placoid interneuron infarction with periarterial sparing reflects MR hypo-oxygenation from misery perfusion involving the entire inner retina (with no OCT angiographic correlate in the acute phase) rather than localized MR/DVC hypoperfusion. Moreover, the fact that ischemia of the SCP is never seen in isolation, but only occurs in association with WIFI/pvPAMM,[10] argues strongly against selective capillary ischemia and in favor of misery perfusion; indeed, there is no relevant anatomical substrate for selective MR ischemia on this scale.

The proponents of pvPAMM were slow to accept that a diminution in AV perfusion pressure across the retinal circulation is capable of generating Paques' plaques whether due to CRVO or partial CRAO (Figures 1 and 4) and that the macular SIR changes in OHM2 and OHM3 have the same physiopathological mechanism as the MR damage in OHM1 and OHM2 (Figure 5).[29] Indeed, although the wider OHM spectrum has recently been acknowledged (in terms of a newly postulated "ischemic cascade"), the fundal features in the exemplar case used to illustrate this cascade were misinterpreted.[32] Thus, there was said to be no sign of SIR ischemia on initial presentation (ie, OHM1), but the presence of axoplasmic sentinels in a characteristic distribution dictates otherwise (ie, OHM2). Confusion has also arisen ever since the term "globular PAMM" was advanced to describe a focal or territorial pattern (as distinct from a watershed or interterritorial pattern) of MR infarction.[33] For example, CRAO with globular PAMM of unspecified origin was recently diagnosed in an eye exhibiting cilioretinal MR infarction,[34] a complication that more likely arose following CRVO.[31]

Finally, it is currently fashionable to describe macular MR infarction with periarterial sparing (as seen in OHM1 and OHM2) in the following terms- a "remarkable" and/or "precise", fern-like, perivenular pattern of PAMM.[29,30,32,35] As illustrated in Figures 3, 4, 5, and 6, however, this is not an accurate portrayal of the geometric ischemic geography. Supporting evidence for such a vein-dominated mechanism (ie, a failure of tissue oxygenation normally provided by the veins) is said to derive from capillary tracing experiments in pig retinae.[36] Thus, a "serial organization of the retinal capillary plexus" is claimed, resulting in a "venular" DCP through which substantially oxygen-desaturated blood flows, even in physiological conditions.[30,32]

However, the morphological findings have not been corroborated by endothelial enzyme histochemistry (to differentiate arteriolar from venular capillary segments), and a venular DCP is difficult to reconcile with the presence of diving arterioles and twin inner-retinal peaks on the transretinal pO_2 profile.[7,25] Furthermore, diffusive oxygen shunting will override all such microvascular anatomic considerations while being central to the classical, unadulterated, "misery perfusion" mechanism of OHM whereby downstream tissues are simply starved of oxygen by ongoing oxidative metabolism upstream.

FUNDING/SUPPORT: THE AUTHOR HAS COMPLETED AND SUBMITTED THE ICMJE FORM FOR DISCLOSURE OF POTENTIAL CONflicts of Interest and none were reported. This research did not receive any specific grant from funding agencies in the public, commercial, or not-for-profit sectors.

Financial Disclosures: The author has indicated no financial conflicts of interest.

REFERENCES

1. Oji EO, McLeod D. Partial central retinal artery occlusion. *Trans Ophthalmol Soc U K* 1978;98(1):156–159.
2. McLeod D, Oji EO, Kohner EM, Marshall J. Fundus signs in temporal arteritis. *Br J Ophthalmol* 1978;62(9):591–594.
3. Michaelson IC. Retinal Circulation in Man and Animals. Springfield, IL: Charles C. Thomas; 1954:74–100.
4. McLeod D, Beatty S. Evidence for an enduring ischaemic penumbra following central retinal artery occlusion, with implications for fibrinolytic therapy. *Prog Retin Eye Res* 2015;49:82–119.
5. Pichi F, Morara M, Veronese C, Lembo A, Nucci P, Ciardella AP. Perivenular whitening in central vein occlusion described by fundus autofluorescence and spectral domain optical coherence tomography. *Retina* 2012;32(7):1438–1439.
6. Spaide RF, Klancnik JM, Cooney MJ. Retinal vascular layers imaged by fluorescein angiography and optical coherence tomography angiography. *JAMA Ophthalmol* 2015;133(1):45–50.
7. Campbell JP, Zhang M, Hwang TS, et al. Detailed vascular anatomy of the human retina by projection-resolved optical coherence tomography angiography. *Sci Rep* 2017;7:42201.
8. Hayreh SS. Acute retinal arterial occlusive disorders. *Prog Retin Eye Res* 2011;30(5):359–394.
9. Kurimoto T, Okamoto N, Oku H, et al. Central retinal artery occlusion resembling Purtscher-like retinopathy. *Clin Ophthalmol* 2011;5:1083–1088.
10. Yu S, Pang CE, Gong Y, et al. The spectrum of superficial and deep capillary ischemia in retinal artery occlusion. *Am J Ophthalmol* 2015;159(1):53–63.
11. McLeod D. Why cotton wool spots should not be regarded as retinal nerve fibre layer infarcts. *Br J Ophthalmol* 2005;89(2):229–237.
12. Baron JC, Bousser MG, Rey A, Guillard A, Comar D, Castaigne P. Reversal of focal "misery-perfusion syndrome" by extra-intracranial arterial bypass in hemodynamic cerebral ischemia. A case study with 15O positron emission tomography. *Stroke* 1981;12(4):454–459.
13. Hickam JB, Frayser R. Studies of the retinal circulation in man. Observations on vessel diameter, arteriovenous oxygen difference, and mean circulation time. *Circulation* 1966;33(2):302–316.
14. Krogh A. The number and distribution of capillaries in muscles with calculations of the oxygen pressure head necessary for supplying the tissue. *J Physiol* 1919;52(6):409–415.
15. McLeod D. Krogh cylinders in retinal development, panretinal hypoperfusion and diabetic retinopathy. *Acta Ophthalmol* 2010;88(8):817–835.
16. Astrup J, Siesjö BK, Symon L. Thresholds in cerebral ischemia: the ischemic penumbra. *Stroke* 1981;12(6):723–725.
17. Moustafa RR, Baron JC. Perfusion thresholds in cerebral ischemia. In: Donnan GA, Baron J-C, Davis SM, Sharp FR, eds. The Ischemic Penumbra. Boca Raton, FL: CRC Press; 2007:21–37.
18. Ellsworth ML, Ellis CG, Popel AS, Pittman RN. Role of microvessels in oxygen supply to tissue. *News Physiol Sci* 1994;9(3):119–123.
19. Andrews RM, Griffiths PG, Johnson MA, Turnbull DM. Histochemical localisation of mitochondrial enzyme activity in human optic nerve and retina. *Br J Ophthalmol* 1999;83(2):231–235.
20. Litts KM, Zhang Y, Freund KB, Curcio CA. Optical coherence tomography and histology of age-related macular degeneration support mitochondria as reflectivity sources. *Retina* 2018;38(3):445–461.
21. Browning DJ. Patchy ischemic retinal whitening in acute central retinal vein occlusion. *Ophthalmology* 2002;109(11):2154–2159.
22. Paques M, Gaudric A. Perivenular macular whitening during acute central retinal vein occlusion. *Arch Ophthalmol* 2003;121(10):1488–1491.
23. Sarda V, Nakashima K, Wolff B, Sahel JA, Paques M. Topography of patchy retinal whitening during acute perfused retinal vein occlusion by optical coherence tomography and adaptive optics fundus imaging. *Eur J Ophthalmol* 2011;21(5):653–656.
24. Ames A III. CNS energy metabolism as related to function. *Brain Res Brain Res Rev* 2000;34(1–2):42–68.
25. Linsenmeier RA, Zhang HF. Retinal oxygen: from animals to humans. *Prog Retin Eye Res* 2017;58:115–151.
26. Rahimy E, Sarraf D, Dollin ML, Pitcher JD, Ho AC. Paracentral acute middle maculopathy in nonischemic central retinal vein occlusion. *Am J Ophthalmol* 2014;158(2):372–380.
27. Yu S, Wang F, Pang CE, Yannuzzi LA, Freund KB. Multimodal imaging findings in retinal deep capillary ischemia. *Retina* 2014;34(4):636–646.

28. Rahimy E, Kuehlewein L, Sadda SR, Sarraf D. Paracentral acute middle maculopathy: what we knew then and what we know now. *Retina* 2015;35(10):1921–1930.
29. Ghasemi Falavarjani K, Phasukkijwatana N, Freund KB, et al. En face optical coherence tomography analysis to assess the spectrum of perivenular ischemia and paracentral acute middle maculopathy in retinal vein occlusion. *Am J Ophthalmol* 2017;177(5):131–138.
30. Garrity ST, Paques M, Gaudric A, Freund KB, Sarraf D. Considerations in the understanding of venous outflow in the retinal capillary plexus. *Retina* 2017;37(10):1809–1812.
31. McLeod D. Central retinal vein occlusion with cilioretinal infarction from branch flow exclusion and choroidal arterial steal. *Retina* 2009;29(10):1381–1395.
32. Bakhoum MF, Freund KB, Dolz-Marco R, et al. Paracentral acute middle maculopathy and the ischemic cascade associated with retinal vascular occlusion. *Am J Ophthalmol* 2018;95(11):143–153.
33. Sridhar J, Shahlaee A, Rahimy E, et al. Optical coherence tomography angiography and en face optical coherence tomography features of paracentral acute middle maculopathy. *Am J Ophthalmol* 2015;160(6):1259–1268.
34. Iafe NA, Onclinx T, Tsui I, Sarraf D. Paracentral acute middle maculopathy and deep retinal capillary plexus infarction secondary to reperfused central retinal artery occlusion. *Retin Cases Brief Rep* 2017;11 Suppl 1:s90–s93.
35. Garrity ST, Tseng VL, Sarraf D. Paracentral acute middle maculopathy in a perivenular fern-like distribution with en face optical coherence tomography. *Retin Cases Brief Rep* 2018;12 Suppl 1:s25–s28.
36. Fouquet S, Vacca O, Sennlaub F, Paques M. The 3D retinal capillary circulation in pigs reveals a predominant serial organization. *Invest Ophthalmol Vis Sci* 2017;58(13):5754–5763.